

Laser-induced Structural Modifications inside Glass Using a Femtosecond Laser and a CO₂ Laser

Takuto ASADA^{*1}, Takayuki TAMAKI^{*1}, Masaya NAKAZUMI^{*1}, Etsuji OHMURA^{*2}, and Kazuyoshi ITOH^{*3}

^{*1} Department of Control Engineering, Nara National College of Technology,
Institute of National Colleges of Technology, Japan
22 Yata-cho, Yamatokoriyama, Nara 639-1080, Japan
a0723@stdmail.nara-k.ac.jp

^{*2} Management of Industry and Technology, Graduate School of Engineering, Osaka University
2-1 Yamadaoka, Suita, Osaka 565-0871, Japan

^{*3} Science Technology Entrepreneurship Laboratory (e-square), Graduate School of Engineering, Osaka University
2-1 Yamadaoka, Suita, Osaka 565-0871, Japan

Abstract

In this paper, we present laser-induced structural modifications inside BK7 glass (OHARA, S-BSL7) using a femtosecond laser and a CO₂ laser system. A femtosecond laser has extremely short pulse duration (less than 10⁻¹² sec) and high peak power. When an intense femtosecond laser pulse irradiates inside transparent material, the nonlinear absorption phenomenon generates around the focal spot, and leads to a localized structural modification in the material. Also CO₂ laser can generate the thermal effect around laser-irradiated area. By combining the nonlinear absorption and thermal effect, we develop novel femtosecond laser microprocessing using thermal effect. We found the 2-wavelengths laser microprocessing (TLAM) has the effect of displacing the focal point of femtosecond laser pulse with the increase of the CO₂ laser power. Moreover the TLAM increases heat-affected zone in the unit time than that using single femtosecond laser microprocessing (SFLAM). The processed diameter using TLAM is approximately twice the size of the diameter using SFLAM. The increase of the diameter of structural modifications expands the possibilities of the application to the three dimensional microfabrication inside the transparent material.

DOI: 10.2961/jlmn.2014.02.0017

Keywords: 2-wavelengths laser microprocessing system, femtosecond laser, CO₂ laser, structural modification, surface ablation, internal processing, glass

1. Introduction

Ultrashort laser pulse has great potential for the three-dimensional (3D) microprocessing in transparent material because the pulse has extremely short pulse duration (less than 10⁻¹² sec) and high peak power. When ultrashort laser pulses irradiate inside transparent material, the laser pulses can become high enough to cause localized permanent structural modifications in the material [1, 2]. Papers on the 3D microfabrication inside the transparent material with the structural modification by single femtosecond laser system have been reported. For example, the 3D optical devices such as waveguides [3, 4], couplers [5], lenses [6], and gratings [7, 8, 9, 10] have been fabricated inside various glass materials.

The size of structural modifications in these devices depends on the pulse energy of femtosecond laser. If the diameter of structural modifications is larger than the ordinary size, the possibilities of the application to the 3D microfabrication inside the transparent material will expand (e.g. reduction of processing time). However, in order to obtain large structural modifications, high-energy femtosecond laser is generally required. For example we investigated the relationship between diameter of structural modifications inside BK7 glass and the pulse energy of femtosecond laser by focusing femtosecond laser pulses (wavelength: 1.064 μm, pulse duration: 400 fs, and repetition rate: 1 MHz) with a 0.40-NA (numerical aperture) objective lens. Figure 1 shows the obtained relationship and the primary curve that is calculated from the diameter of pro-

cessed structural modifications. From the primary curve the expected diameter of structural modifications with more than 1.4 μJ in pulse energy of femtosecond laser is estimated and denoted with a dotted line in Fig.1. For example, in order to form the 100 μm diameter of structural modifications, more than 2 μJ in pulse energy of femtosecond laser pulse energy will be required. However, a high-energy femtosecond laser generally needs space and cost for the installation and operation.

In this paper to create large diameter of structural modification using low-energy femtosecond laser (for example up to 1.4 μJ), we propose the 2-wavelengths laser microprocessing (TLAM), which consists of CO₂ laser and femtosecond laser. The CO₂ laser beam has high-power continuous or pulse wave in the infrared region. Therefore the thermal effects will occur in the laser-irradiated area

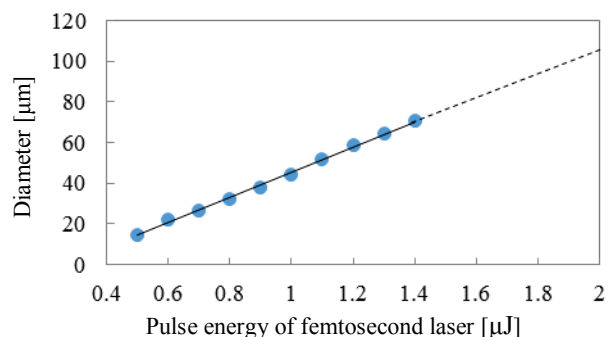


Fig. 1 Relationship between diameter of structural modifications inside BK7 glass and pulse energy of femtosecond laser.

[11, 12, 13, 14]. By use of the thermal effect with CO₂ laser and the nonlinear phenomenon with femtosecond laser, TLAM is developed.

2. Principle of TLAM

2.1 The processed amount inside glass using TLAM or FSLAM

Figure 2 shows the schematic diagram of single femtosecond laser microprocessing (FSLAM) and the 2-wavelengths laser microprocessing (TLAM). In order to investigate the effect of FSLAM and TLAM, femtosecond laser pulses without/with CO₂ laser beam irradiate inside BK7 glass (200 μm depth from glass surface). When femtosecond laser pulses irradiate transparent material, the laser-induced structural modifications are created around focal spot through the nonlinear and avalanche ionization phenomenon. By providing the energy of CO₂ laser beam to the material with the irradiation of femtosecond laser, we consider that the avalanche ionization is likely to occur [15]. Therefore the diameters of the laser-induced structural modifications using TLAM will be larger than that using FSLAM. Thus the heat-affected zone in the unit time using TLAM increases than that using FSLAM.

2.2 Displacement of focal position

When femtosecond laser pulses irradiate on the surface of transparent material, the pulse causes ablation around the focal spot. However, when CO₂ laser beam and femtosecond laser pulses irradiate on the surface of the material simultaneously, internal processing is realized because the movement of the focal point occurs. Although the mechanism about the movement is still under investigation, we consider that the factor is probably thermal lens effect and/or thermal expansion of the glass.

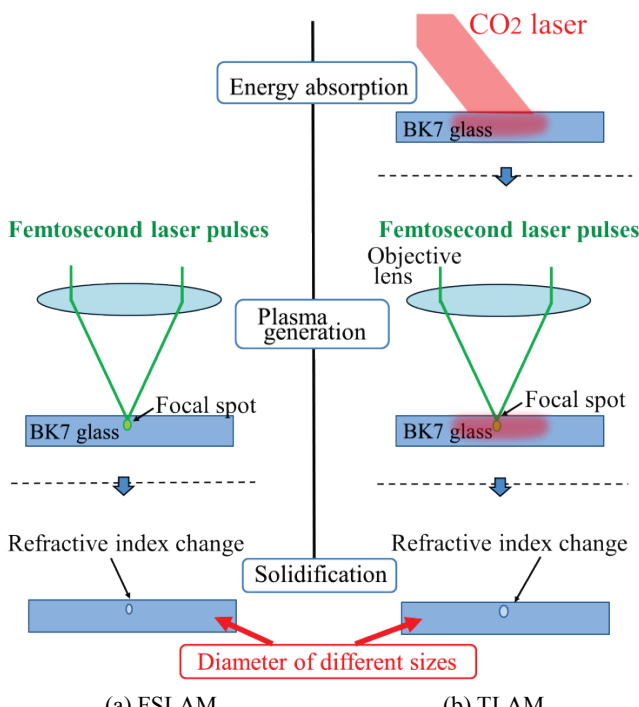


Fig. 2 The schematic diagram of FSLAM and TLAM.

3. Experimental setup

Figure 3 shows an optical setup for the 2-wavelengths laser microprocessing (TLAM) that consists of femtosecond fiber laser and CO₂ laser systems. A femtosecond fiber laser system (Fianium, FP1060S-PP-D) generates 1.064 μm, 400 fs, and 1 MHz ultrafast laser pulses with pulse energy up to 2 μJ (immediately after output of laser system). It should be noted that the 1 MHz-repetition-rate leads to the heat accumulation in BK7 glass (OHARA, S-BSL7, specifications of the glass are shown in Table 2 [15]). Also CO₂ laser system (Kantum Electronics, H48-1-28SW) generates pulsed laser beam with a repetition rate of 5 kHz and a wavelength of 10.6 μm. CO₂ laser beam was irradiated to glass for 5 seconds in order to provide a sufficient heat effect. Next femtosecond laser pulses were irradiated simultaneously behind the CO₂ laser irradiation. The pulse energy of femtosecond laser was controlled by rotating a half-wave plate in front of a Glan-laser polarizer. The output power was controlled by the duty ratio of electrical pulse in the CO₂ laser driver. Table 3 shows the beam size of the CO₂ laser beam with different laser output. The sample to be processed was fixed a computer-controlled three-dimensional stage. Femtosecond laser pulses were focused on the glass surface or inside glass with a 20× objective lens (Olympus LMPlan 20×IR) of a 0.40 numerical aperture. By translating the glass sample perpendicular to the optical axis of femtosecond laser pulses with a distance of 1 mm, the linear structural modification regions were created. The laser-induced modification region were observed in the xy-plane and in the xz-plane by optical transmission microscopes with white-light illumination.

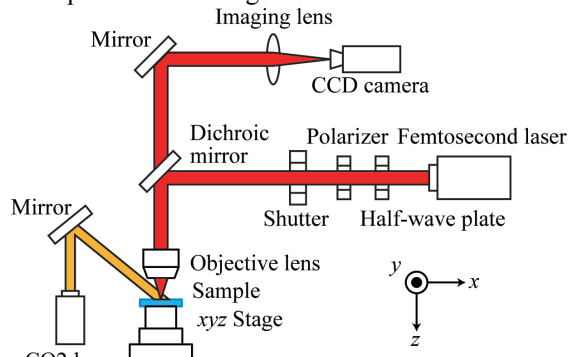


Fig. 3 Schematic diagram of optical setup used for TLAM using femtosecond laser and CO₂ laser systems. CCD: charge-coupled device camera.

Table 1 Characteristics of S-BSL 7 glass [16].

Dimension [mm]	5 × 30
Thickness [mm]	0.67
Refractive index [-]	1.51
Transition point [°C]	576
Softening point [°C]	718
Coefficient of thermal conductivity [W/m·K]	1.13
Strain point [°C]	532
Annealing point [°C]	563
Deformation point [°C]	625
Coefficient of linear expansion [-30~70 °C]	72

[10 ⁻⁷ /°C]	100~300 [°C]	86
Table 2 The beam size of the CO ₂ laser beam.		
CO ₂ laser output [W]	The laser beam diameter [mm]	
2	8.5	
3	9.5	
4	10.0	

4. Results and discussions

4.1 Surface ablation

4.1.1 Morphology dependence on the thermal effect of CO₂ laser beam

In order to clarify the influence of the thermal effect of the CO₂ laser beam, we demonstrated laser microprocessing of BK7 glass by using (i) single femtosecond laser microprocessing (FSLAM) or (ii) the 2-wavelengths laser microprocessing (TLAM). The pulse energy of femtosecond laser was set to 0.6 μJ. The output power of CO₂ laser was set to 3 W. Figures 4(a) and (b) show optical microscope images of laser-induced structural modification in BK7 glass using FSLAM and TLAM, respectively. From Figs. 4(a) and (b), the laser-induced structural modification is surface ablation for FSLAM, and that is refractive-index change inside glass for TLAM.

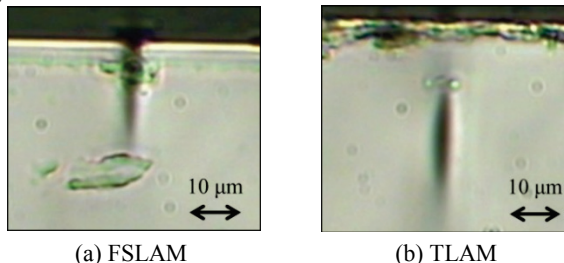


Fig. 4 Optical microscope images of laser-induced structural modification in BK7 glass using (a) FSLAM and (b) TLAM, respectively.

4.1.2 Morphology dependence on output power of CO₂ laser beam and/or energy of femtosecond laser pulses

We investigated the laser-induced morphology (surface ablation, internal processing, and intermediate state (i.e. surface ablation region changed to internal processing during laser processing)) in BK7 glass by changing the output power of CO₂ laser beam and/or energy of femtosecond laser pulses. Figure 5 shows the examples of surface ablation and internal processing in the laser-induced morphology. The pulse energy of femtosecond laser was changed to 0.60 μJ, 0.65 μJ, 0.70 μJ, and 0.75 μJ. The output power of CO₂ laser beam was also changed to 1 W, 2 W, 3 W, and 4 W. Table 4 shows the laser-induced morphology in each condition. In Table 4, open circle (○), cross mark (×), and open square (□) show internal processing, surface ablation, and intermediate state, respectively. From Table 4 we confirm that the laser-induced morphologies are internal processing or intermediate state with more than 2 W output power of CO₂ laser beam. Note that, with more than 5 W output power of CO₂ laser beam, the BK7 glass

sample physically broke. Therefore the morphology depends on the power of CO₂ laser beam.

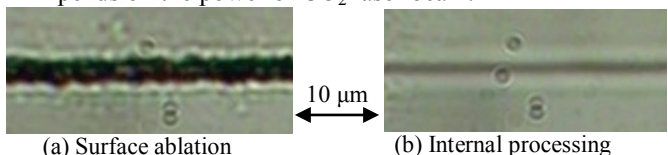


Fig. 5 Examples of surface ablation and internal processing in the laser-induced morphology.

Table 3 The laser-induced morphology in each condition. Open circle (○), cross mark (×), and open square (□) show internal processing, surface ablation, and intermediate state, respectively.

Power of CO ₂ laser beam [W]	0	1	2	3	4
Energy of femtosecond laser pulses [μJ]					
0.60	×	×	○	○	○
0.65	×	×	○	○	○
0.70	×	□	○	○	○
0.75	×	×	□	○	○

4.1.3 Depth dependence of laser-induced morphology on output power of CO₂ laser beam and/or energy of femtosecond laser pulses

We investigated the depth of laser-induced morphology from the glass surface by changing the output power of CO₂ laser beam and/or energy of femtosecond laser pulses. The pulse energy of femtosecond laser was changed to 0.60 μJ, 0.65 μJ, 0.70 μJ, and 0.75 μJ. The output power of CO₂ laser beam was also changed to 1 W, 2 W, 3 W, and 4 W. Figure 6 shows the cross section of a laser-induced morphology and definition of depth in the morphology. Also Fig. 7 shows relationship between the depth of the morphology and the power of CO₂ laser beam. From Fig. 7 the depth is increased with an increase in the power of CO₂ laser beam. About the dependence of the depth on the energy of femtosecond laser pulses, in the region of internal processing, the depth depends on the energy of femtosecond laser pulse. In contrast, in the region of surface ablation, the depth doesn't depend on the energy.

We consider that the reason for the dependence of the depth on output power of CO₂ laser beam and energy of femtosecond laser pulses is likely the thermal effect that is described in Section 2. The generation of the thermal effect is shown during laser microprocessing using TLAM (see Fig. 8). From Fig. 8 we confirm that the image during processing is blurred. The reason is likely thermal expansion due to the increase of temperature with energy absorption of CO₂ laser beam into the glass although we will investigate the mechanism on the displacement of focal position in detail in the future.

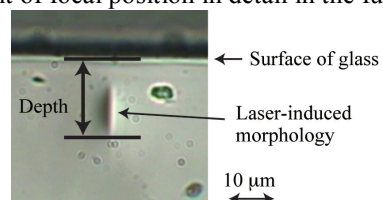


Fig. 6 Cross section of laser-induced morphology and definition of depth in the morphology.

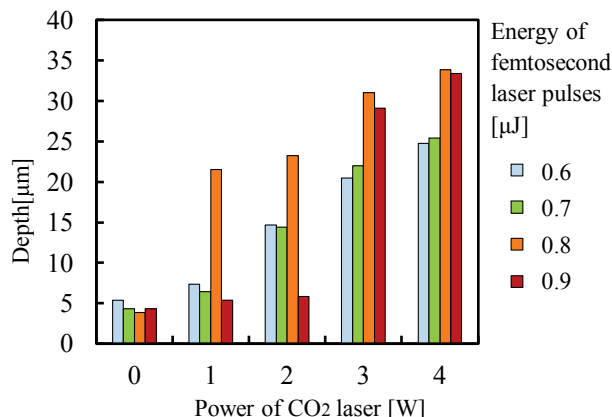


Fig. 7 Relationship between the depth of the morphology and the power of CO₂ laser beam.

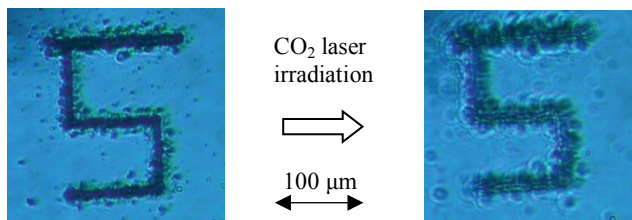


Fig. 8 Thermal effect during laser microprocessing using CO₂ laser

4.1.4 Dependence of laser-induced structural modifications on scan speeds

The purpose in this section is to clarify the dependence of laser-induced structural modifications inside BK7 glass on scan speeds by using TLAM. By translating the glass sample perpendicular to the optical axis of femtosecond laser pulses with a distance of 1 mm, the linear structural modification regions were created. The dependence of laser-induced structural modifications on scan speeds was investigated by changing scan speed from 0.1 mm/s to 1.0 mm/s at an interval of 0.1 mm/s. The output power was also changed to 1 W, 2 W, and 3 W. Table 5 shows the laser-induced morphology in each condition at intervals of 0.2 mm/s. In Table 5, open circle (○) and cross mark (×) show internal processing and surface ablation, respectively. From Table 5 the laser-induced morphologies are internal processing in either case of the CO₂ laser output is 2 W and scan speed is less than 0.6 mm/s or CO₂ laser output is 3 W. The laser-induced morphologies are surface ablation in either case of the CO₂ laser output is 2 W and scan speed is more than 0.8 mm/s or CO₂ laser output is 1 W. From these results we assume that it is an internal processing when the thermal effects are given enough.

Table 4 The laser-induced morphology in each condition. Open circle (○) and cross mark (×) show internal processing and surface ablation, respectively.

CO ₂ laser power [W]	Scan speed [mm/s]				
	0.2	0.4	0.6	0.8	1.0
1	×	×	×	×	×
2	○	○	○	×	×
3	○	○	○	○	○

4.2 Internal processing

4.2.1 The effect of CO₂ laser beam for the laser-induced morphology inside glass

In order to reveal the effect by CO₂ laser beam in TLAM, we demonstrated the laser microprocessing of BK7 glass using FSLAM or TLAM. The pulse energy of femtosecond laser was set to 1.3 μJ. The output power of CO₂ laser power was set to 5 W. Irradiation time of femtosecond laser was 0.05 sec and that of CO₂ laser was 5 sec. Figures 9(a) and (b) show optical images of processed material using FSLAM and TLAM, respectively. From Figs. 9(a) and (b), both of FSLAM and TLAM resulted in refractive index change inside glass. The diameter of the refractive index change region using TLAM is twice that using FSLAM.

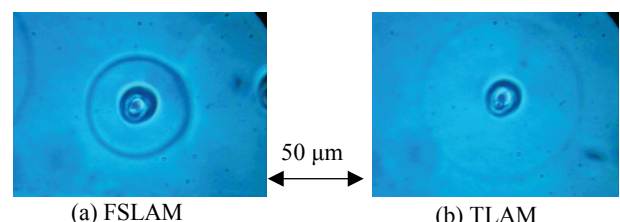


Fig. 9 Optical images of processed material using (a) FSLAM or (b) femtosecond and CO₂ laser systems (TLAM).

4.2.2 Dependence of diameter and magnification of the laser-induced structural modifications on output power of CO₂ laser beam and energy of femtosecond laser pulses

We investigated the diameter and magnification of the structural modifications by changing the output power of CO₂ laser beam and/or energy of femtosecond laser pulses. The pulse energy of femtosecond laser was changed from 0.8 μJ to 1.3 μJ at an interval of 0.1 μJ. The output power of CO₂ laser beam was also changed from 0 W to 5 W at an interval of 1 W. Figure 10 shows the examples of the change in the diameter of the refractive index change region when the pulse energy of femtosecond laser was set to 1.3 μJ. Figure 11 shows the diameter of the refractive index change region in each condition. Figure 12 shows the magnification of the diameter of the refractive index change region using TLAM compared with that using FSLAM. Magnification is calculated from formula (1). In Fig. 12 the increasing rate of magnification in the higher energy of femtosecond laser (e.g., 1.2 μJ and 1.3 μJ) is bigger than that in the smaller that (e.g., 0.8 μJ and 0.9 μJ). From Fig. 11 and Fig. 12, we confirmed that TLAM increased heat-affected zone in the unit time than that using FSLAM. The processed diameter using TLAM is twice the size of the diameter using FSLAM.

$$\text{Magnification} = \frac{\text{The diameter using TLAM}}{\text{The diameter using FSLAM}} \quad (1)$$

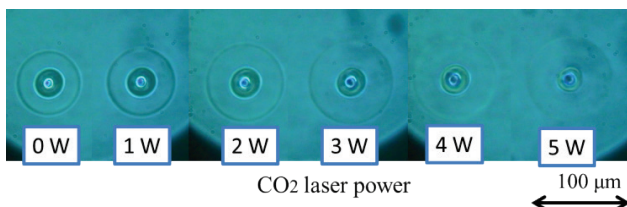


Fig. 10 Dependence of the diameter of refractive index change region on CO₂ laser power.

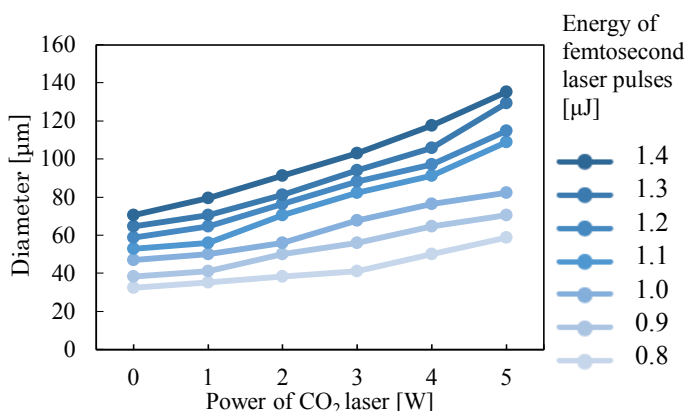


Fig. 11 The diameter of the refractive-index change region by changing the output power of CO₂ laser beam and/or energy of femtosecond laser pulses.

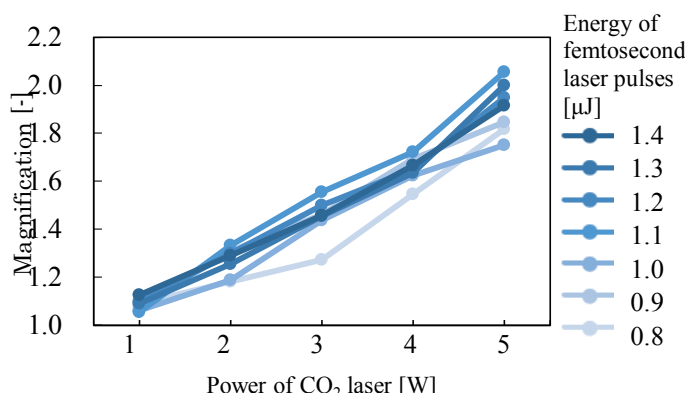


Fig. 12 The magnification of the diameter of the refractive-index change region by changing the output power of CO₂ laser beam and/or energy of femtosecond laser pulses.

Conclusion

We have investigated the laser-induced structural modifications in a BK7 glass sample (OHARA, S-BSL7) using a high-repetition-rate femtosecond fiber laser and a CO₂ laser system. For the depth dependence of laser-induced morphology on output power of CO₂ laser beam and/or energy of femtosecond laser pulses, the depth is increased with an increase in the power of CO₂ laser beam and the energy of femtosecond laser pulses except the region of surface ablation. This results show that the laser microprocessing using femtosecond and CO₂ laser systems is possible to change the laser-induced morphology of BK7 glass. Also we have investigated internal processing in BK7 glass with the 2-wavelengths laser microprocessing(TLAM) using femtosecond laser system and CO₂ laser system. The diameter of the refractive-index change region changed by changing the out-

put power of CO₂ laser beam and/or energy of femtosecond laser pulses. The diameter of the refractive index change region using TLAM is approximately twice the size of the diameter using single femtosecond laser microprocessing (SFLAM). The increase of the diameter of structural modifications expands the possibilities of the application to the three dimensional microfabrication inside the transparent material.

References

- [1] K. Itoh, W. Watanabe, S. Nolte, and C. B. Schaffer, "Ultrafast processes for bulk modification of transparent materials," *MRS Bulletin*, 31 (2006) 620-625.
- [2] M. Shimizu1, M. Sakakura, M. Ohnishi, Y.Shimotsuma, T. Nakaya, K. Miura1, and Kazuyuki Hirao, "Mechanism of heat-modification inside a glass after irradiation with high-repetition rate femtosecond laser pulses,"
- [3] K. M. Davis, K. Miura, N. Sugimoto, and K. Hirao, "Writing waveguides in glass with a femtosecond laser," *Opt. Lett.*, 21 (1996) 1729-1731.
- [4] K. Yamada, W. Watanabe, T. Toma, K. Itoh, and J. Nishii, "*In situ* observation of photoinduced refractive-index changes in filaments formed in glasses by femtosecond laser pulses," *Opt. Lett.*, 26 (2001) 19-21.
- [5] D. Homoelle, S. Wielandy, A. L. Gaeta, N. F. Borrelli, and C. Smith, "Infrared photosensitivity in silica glasses exposed to femtosecond laser pulses," *Opt. Lett.*, 24, (1999) 1311-1313.
- [6] K. Yamada, W. Watanabe, Y. Li, K. Itoh, and J. Nishii, "Multilevel phase-type diffractive lenses in silica glass induced by filamentation of femtosecond laser pulses," *Opt. Lett.*, 29 (2004) 1846-1848.
- [7] L. Sudrie, M. Franco, B. Prade, and A. Mysyrowicz, "Writing of permanent birefringent microlayers in bulk fused silica with femtosecond laser pulses," *Opt. Commun.*, 171 (1999) 279-284.
- [8] K. Yamada, W. Watanabe, K. Kintaka, J. Nishii, and K. Itoh, "Volume grating induced by a self-trapped long filament of femtosecond laser pulses in Silica Glass" *Jpn. J. Appl. Phys.*, **42** (2003) 6916-6919.
- [9] K. Kawamura, N. Sarukura, M. Hirano, and H. Hosono, "Holographic encoding of fine-pitched micrograting structures in amorphous SiO₂ thin films on silicon by a single femtosecond laser pulse," *Appl. Phys. Lett.*, **78** (2001) 1038-1341.
- [10] Y. Li, W. Watanabe, K. Yamada, T. Shinagawa, K. Itoh, J. Nishii, and Y. Jiang, "Holographic fabrication of multiple layers of grating inside soda-lime glass with femtosecond laser pulses," *Appl. Phys. Lett.*, **80** (2002) 1508-1511.
- [11] J. P. Gordon, R. C. C. Leite, R. S. Moore, S. P. S. Porto, and J. R. Whinnery, "Long-transient effects in lasers with inserted liquid samples," *J. Appl. Phys.*, 36 (1965) 3-8.
- [12] Terazima, M., Horiguchi, M., and Azumi, T., *Anal. Chem.* 61, (1989) 883-888.
- [13] T.M.A., Rasheed, K.P.B., Moosad, V.P.N., Nampoori and K.Sathianandan *Spectro. Chim. Acta.A*, 43, (1973) 72.

- [14] P.E.Dyer, I.Waldeck, G.C. Roberts, J.Phys. D.Appl., Phys. 30, (1997) 19.
- [15] A. Brodeur and S.L. Chin, "Ultrafast white-light continuum generation and self-focusing in transparent condensed media," JOSA B 16 (1999) 637-650.
- [16] http://www.ohara-gmbh.com/e/katalog/d_s-bsl7_e.html

(Received: July 25, 2013, Accepted: May 14, 2014)